PHYSICAL REVIEW D **96,** 035020 (2017)

Revisiting vectorlike quark models with enhanced top Yukawa coupling

Michio Hashimoto

Chubu University, 1200 Matsumoto-cho, Kasugai-shi, Aichi 487-8501, Japan

(Received 18 April 2017; published 23 August 2017)

We revisit a scenario with an enhanced top Yukawa coupling in vectorlike quark (VLQ) models, where the top Yukawa coupling is larger than the standard model value and the lightest VLQ has a negative Yukawa coupling. We find that the parameter space satisfying the LHC bounds of the Higgs signal strengths consistently with the precision measurements is rather wide. Because the Lagrangian parameters of the Yukawa couplings are large, such scenario can be realized in some strongly interacting theories. It also turns out that there is a noticeable relation between the contributions of the triangle and box diagrams in the $gg \to hh$ process by using the lowest order of the $1/M$ expansion where M is the heavy mass running in the loops.

DOI: 10.1103/PhysRevD.96.035020

I. INTRODUCTION

The LHC experiments have discovered a Higgs boson and revealed that its properties are similar to that of the standard model (SM) [1]. It is thus essential to explore any signatures of physics beyond the SM (BSM). One of the hint is that the observed signal strength of $pp \to t\bar{t}h$ channel is deviated from the SM value about twice, $\mu_{tth} = 2.3^{+0.7}_{-0.6}$ for the Run 1 combined data [1], $\mu_{tth} = 1.8^{+0.7}_{-0.7}$ for the ATLAS Run 2 [2], and $\mu_{tth} = 1.5^{+0.5}_{-0.5}$ for the CMS Run 2 in the multilepton final states[1] [6], although the uncertainties are still large.

These experiments provide a reason for considering models based on strongly interacting theories. In this direction,[2] widely studied are vectorlike quark (VLQ) models [9–19], the minimal composite Higgs models (MCHMs) [20,21], and the Little Higgs models [22,23]. We easily find, however, the top Yukawa coupling is always suppressed in the VLQ model having only one up-type quark [13]. For example, introducing the VLQ $U_{L,R}$ having $+2/3$ electric charge as in the top-seesaw model [24], the top Yukawa coupling is modified as $c_L^2 g_{tth}^{\rm SM}$, where $c_L \equiv \cos\theta_L$ represents the cosine of the mixing angle between t_L and U_L, and we defined the SM top Yukawa coupling by $g_{tth}^{\rm SM} = m_t/v$ with m_t and v being the top mass and the vacuum expectation value (VEV) of the Higgs field, respectively. It is the case[3] for the MCHMs such as MCHM4, MCHM5, and MCHM10 where the fermions are embedded in the spinorial, 5, and 10 representations of $SO(5)$, respectively [26,27]. Nevertheless one should not jump to a conclusion: A simple model is effective for a benchmark, but it might be misguided if simplified too much.

In this paper, we reconsider a scenario that the top Yukawa coupling is larger than the SM value by $\mathcal{O}(10\%)$, and the lightest VLQ with the mass around 1 TeV has a negative Yukawa coupling of the order of $-m_t/v$, introducing more than one up-type VLQ [16,17,28]. In our scenario, owing to the cancellation among the Yukawa couplings, the Higgs signal strengths can be consistent with the experiments. A similar analysis[4] was performed in Ref. [17]. Although the allowed region looked narrow in Ref. [17], we find that our scenario is possible in a rather wide parameter space.

We numerically show that our scenario is realized, roughly speaking, when the Lagrangian parameters y_{ij} of the Yukawa interactions are large, say, $|y_{ij}| \gtrsim 2$. This may suggest the existence of the underlying strongly interacting models where the dynamically generated Yukawa couplings are typically around $3 \sim 5$ [24]. As for the di-Higgs production process $gg \to hh$ [32–39], we find a noticeable relation between the contributions of the triangle and the box diagrams in the lowest order of the $1/M$ expansion, where M is the relevant heavy mass running in the loops. The di-Higgs production process may give information on the off-diagonal Yukawa couplings.

The paper is organized as follows: In Sec. II, we introduce the VLQ model. In Sec. III, we first describe the existence proof of our scenario in an analytical approach, and next show a numerical calculation. Section IV is devoted to

[1] A combined result of the CMS Run 2 has not yet been reported. For other decay channels, $\mu_{tth} = 1.91^{+1.5}_{-1.2}$ in the $h \to \gamma\gamma$ decay channel [3], $\mu_{tth} = -0.19^{+0.80}_{-0.81}$ in the $h \to b\bar{b}$ decay channel [4], and $\mu_{tth} = 0.00^{+1.19}_{-0.00}$ in the $h \to ZZ \to 4\ell$ channel [5].

[2] Although the top condensate model [7] and the chiral fourth generation [8] directly predict large Yukawa couplings, they had been severely constrained.

[3] Quite recently, it is shown that the MCHMs with the fermions of the $\mathbf{5} + \mathbf{10}$ or $\mathbf{14}$ representations can have the enhanced or suppressed tth coupling [25].

[4] In the framework of the two Higgs doublet model, the cancellation mechanism via the light stop was considered in Ref. [29,30]. See also Ref. [31].

summary. In Appendix A, the oblique parameters [40] in our model are presented. Analytical expressions of the triangle and the box contributions to the $gg \to hh$ process in the lowest order of the $1/M$ expansion are given in Appendix B.

II. VECTORLIKE QUARK MODEL

Let us introduce two types of the VLQ's, $U_{L,R}$ and $Q_{L,R} = (X, T)_{L,R}$, having the hypercharges $\frac{2}{3}$ and $\frac{7}{6}$, respectively. (See also Table I.) Because of no mixing between the bottom quark and VLQ's, the flavor constraints such as $Z \to b\bar{b}$, etc. can be suppressed in this model. Assuming one Higgs doublet model, the mass terms and the Yukawa interactions are

$$\mathcal{L}_Y = -y_{13}\bar{q}_L\tilde{H}U_R - y_{21}\bar{Q}_L H t_R - y_{23}\bar{Q}_L H U_R - y_{32}\bar{U}_L H^\dagger Q_R + (\text{H.c.}), \tag{1}$$

$$\mathcal{L}_{\text{VM}} = -m_{22}\bar{Q}_L Q_R - m_{33}\bar{U}_L U_R - m_{31}\bar{U}_L t_R + (\text{H.c.}), \tag{2}$$

with $q_L = (t, b)_L$, and $\tilde{H} \equiv i\tau_2 H^*$. The SM term of $y_{11}\bar{q}_L\tilde{H}t_R$ was rotated away via the t_R–U_R mixing like in the top seesaw model [24], while m_{31} is removed in literature [16,17]. We here abbreviated the SM part such as the light quark sector, gauge kinetic terms, etc.

After the electroweak symmetry breaking (EWSB), the mass matrix is then

$$\mathcal{L}_M = -(\bar{t}_L\bar{T}_L\bar{U}_L)\mathcal{M}\begin{pmatrix} t_R \\ T_R \\ U_R \end{pmatrix} - m_{22}\bar{X}_L X_R \tag{3}$$

with $\langle H \rangle = (0, \frac{v}{\sqrt{2}})^T$, $v = 246$ GeV, and

$$\mathcal{M} \equiv \frac{v}{\sqrt{2}}\mathbf{Y} \oplus \mathbf{M} = \frac{v}{\sqrt{2}}\begin{pmatrix} 0 & 0 & y_{13} \\ y_{21} & 0 & y_{23} \\ 0 & y_{32} & 0 \end{pmatrix} + \begin{pmatrix} 0 & 0 & 0 \\ 0 & m_{22} & 0 \\ m_{31} & 0 & m_{33} \end{pmatrix}, \tag{4}$$

TABLE I. Charge assignment of the VLQ model.

	$SU(3)_c$	$SU(2)_W$	$U(1)_Y$
$q_L = (t, b)_L$	**3**	**2**	$\frac{1}{6}$
t_R	**3**	**1**	$\frac{2}{3}$
b_R	**3**	**1**	$-\frac{1}{3}$
$Q_{L,R} = (X, T)_{L,R}$	**3**	**2**	$\frac{7}{6}$
$U_{L,R}$	**3**	**1**	$\frac{2}{3}$

where the mass of the X quark with $+5/3$ electric charge is not affected by the EWSB, i.e., $M_X = m_{22}$. We diagonalize $\mathcal{M}$ by

$$\mathcal{M}_{\text{diag}} = V_L^\dagger \mathcal{M} V_R, \qquad \mathcal{M}_{\text{diag}} = \text{diag}(m_1, m_2, m_3), \tag{5}$$

with $0 \le m_1 \le m_2 \le m_3$, and

$$\begin{pmatrix} t_{L,R} \\ T_{L,R} \\ U_{L,R} \end{pmatrix} = V_{L,R}\begin{pmatrix} t'_{L,R} \\ T'_{L,R} \\ U'_{L,R} \end{pmatrix}, \tag{6}$$

where $(t, T, U)_{L,R}$ and $(t', T', U')_{L,R}$ represent the gauge and mass eigenstates, respectively. Each up-type quark mass is identified by $m_t = m_1$, $M_T = m_2$, and $M_U = m_3$. The Yukawa coupling matrix $\mathbf{G}^h$ in the mass eigenstates is given by

$$\mathcal{L}_Y = -h(\bar{t}'_L\bar{T}'_L\bar{U}'_L)\mathbf{G}^h\begin{pmatrix} t'_R \\ T'_R \\ U'_R \end{pmatrix}, \tag{7}$$

with

$$\mathbf{G}^h = \frac{1}{\sqrt{2}}V_L^\dagger \mathbf{Y} V_R. \tag{8}$$

III. ANALYTICAL AND NUMERICAL STUDIES

A. Analytical study with crude approximation

We schematically show our scenario having $\mathbf{G}^h_{11} > m_t/v$ and $\mathbf{G}^h_{22} < 0$ is possible in an analytical approach. For this purpose, we employ a crude approximation in this subsection. A numerical study without such approximation will be shown in the next subsection.

Let us take the mass matrix as a symmetric one,

$$\mathcal{M} = M_X\begin{pmatrix} 0 & 0 & \epsilon \\ 0 & 1 & \xi \\ \epsilon & \xi & a \end{pmatrix}, \tag{9}$$

where we scaled the mass matrix by $M_X = m_{22}$. For the perturbation theory, the parameters arising from the Yukawa couplings should not be so large, i.e., ϵ^2, $\xi^2 \ll 1$. We also assume $a \ge 1$. We diagonalize $\mathcal{M}$ by the matrices of

$$V_L = (\vec{v}_t\vec{v}_T\vec{v}_U), \qquad V_R = (-\vec{v}_t\vec{v}_T\vec{v}_U) = V_L\text{diag}(-1, 1, 1), \tag{10}$$

where the first, the second and the third components (v_{t1}, v_{T2} and v_{U3}) of $\vec{v}_t$, $\vec{v}_T$ and $\vec{v}_U$ are order of unity,

$$v_{t1} \equiv \vec{v}_t^{(1)} = \mathcal{O}(1), \qquad v_{T2} \equiv \vec{v}_T^{(2)} = \mathcal{O}(1), \qquad v_{U3} \equiv \vec{v}_U^{(3)} = \mathcal{O}(1), \tag{11}$$

respectively, and then obtain the mass eigenvalues,

$$\frac{m_t}{M_X} \equiv \lambda_1 = \mathcal{O}\left(\frac{\epsilon^2}{a}\right), \qquad \frac{M_T}{M_X} \equiv \lambda_2 < 1, \qquad \frac{M_U}{M_X} \equiv \lambda_3 > a. \tag{12}$$

In general, by taking the trace and the determinant, we find

$$-\lambda_1 + \lambda_2 + \lambda_3 = 1 + a, \qquad \lambda_1\lambda_2\lambda_3 = \epsilon^2, \qquad -G^h_{tt} + G^h_{TT} + G^h_{UU} = 0, \tag{13}$$

where we defined the diagonal components of the Yukawa couplings in the mass basis as $\mathbf{G}^h_{11,22,33} \equiv G^h_{tt,TT,UU}$. More explicitly, the Yukawa couplings of G^h_{tt} and G^h_{TT} are given by

$$G^h_{tt} = \frac{m_t}{v}\left[1 + \frac{v_{t1}^2}{(1+\lambda_1)\epsilon^2}\{(a\lambda_1 - \epsilon^2)(2+\lambda_1) + \lambda_1^2\}\right], \tag{14}$$

$$G^h_{TT} = -(1-\lambda_2)\frac{M_X}{v}\left[1 + \frac{(1-\lambda_2)(a-\lambda_2)}{\xi^2}\right]v_{T2}^2 < 0, \tag{15}$$

and the situation of $G^h_{tt} > m_t/v$ is realized when

$$\xi^2 > \frac{1+\lambda_0}{2}(\epsilon^2 - (a-1)\lambda_0), \tag{16}$$

with

$$\lambda_0 \equiv \frac{4\epsilon^2}{2a - \epsilon^2 + \sqrt{(2a-\epsilon^2)^2 + 8\epsilon^2(1+a)}}. \tag{17}$$

An analytic solution is frequently useful. Let us take $\xi = \frac{\epsilon}{a}\sqrt{a+\epsilon^2}$, for example. In this case, we find that the eigenvalues are

$$\lambda_1 = \frac{\epsilon^2}{a}, \qquad \lambda_2 = 1 - \delta^2, \qquad \lambda_3 = a + \frac{\epsilon^2}{a} + \delta^2, \tag{18}$$

with

$$\delta^2 \equiv \frac{2\epsilon^2}{a(a-1) + \epsilon^2 + \sqrt{\{a(a-1)+\epsilon^2\}^2 + 4a\epsilon^2}}, \tag{19}$$

and the corresponding eigenvectors are

$$\vec{v}_t = v_{t1}\begin{pmatrix} 1 \\ \frac{\epsilon^2}{a\sqrt{a+\epsilon^2}} \\ -\frac{\epsilon}{a} \end{pmatrix}, \qquad \vec{v}_T = v_{T2}\begin{pmatrix} -\frac{\lambda_3\delta^2}{\sqrt{a+\epsilon^2}} \\ 1 \\ -\frac{\epsilon}{(\lambda_3-1)\sqrt{a+\epsilon^2}} \end{pmatrix},$$
$$\vec{v}_U = v_{U3}\begin{pmatrix} \frac{\epsilon(1-\delta^2)}{a} \\ \frac{\epsilon\sqrt{a+\epsilon^2}}{a(\lambda_3-1)} \\ 1 \end{pmatrix}, \tag{20}$$

with

$$v_{t1}^{-1} = \sqrt{1 + \frac{\epsilon^2(a+2\epsilon^2)}{a^2(a+\epsilon^2)}}, \tag{21}$$

$$v_{T2}^{-1} = \sqrt{1 + \frac{\delta^4(a^2+\epsilon^2\lambda_3^2)}{\epsilon^2(a+\epsilon^2)}}, \tag{22}$$

$$v_{U3}^{-1} = \sqrt{1 + \frac{\epsilon^2}{a^2}\left((1-\delta^2)^2 + \frac{a+\epsilon^2}{(\lambda_3-1)^2}\right)}. \tag{23}$$

The following relations might be useful:

$$(1-\lambda_2)(\lambda_3-1) = \delta^2(\lambda_3-1) = \frac{\epsilon^2}{a}, \quad \lambda_2\lambda_3 = \lambda_3(1-\delta^2) = a. \tag{24}$$

Substituting the above results for Eqs. (13)–(15), we explicitly obtain

$$G^h_{tt} = \frac{m_t}{v}\left[1 + \frac{a\epsilon^2}{a^3 + a(a+1)\epsilon^2 + 2\epsilon^4}\right] > \frac{m_t}{v}, \tag{25}$$

$$G^h_{TT} = -\frac{M_X}{v}\delta^2\left(2 - \frac{a\delta^2 + \epsilon^2}{a+\epsilon^2}\right)v_{T2}^2 < 0, \tag{26}$$

$$G^h_{UU} = G^h_{tt} - G^h_{TT}. \tag{27}$$

In this way, our scenario can be realized in the framework of the VLQ model. The parameter space should be constrained by the S and T-parameters, however.

B. Numerical study without approximation

Without assuming the symmetric mass matrix (9), we now calculate numerically the signal strengths in our model:

$$\mu_F^{VV} \equiv \mu^{VV}_{\mathrm{ggF+ttH}} = \frac{(\sigma_{ggF} + \sigma_{ttH})\mathrm{Br}^{VV}}{(\sigma_{ggF} + \sigma_{ttH})_{\mathrm{SM}}\mathrm{Br}^{VV}_{\mathrm{SM}}} \simeq \kappa_g^2, \tag{28}$$

$$\mu_F^{\gamma\gamma} \equiv \mu^{\gamma\gamma}_{\mathrm{ggF+ttH}} = \frac{(\sigma_{ggF} + \sigma_{ttH})\mathrm{Br}^{\gamma\gamma}}{(\sigma_{ggF} + \sigma_{ttH})_{\mathrm{SM}}\mathrm{Br}^{\gamma\gamma}_{\mathrm{SM}}} \simeq \kappa_g^2\kappa_\gamma^2, \tag{29}$$

where $VV = WW$ and ZZ, and the scaling factors $\kappa_{g,\gamma,f}$ are defined by

$$\kappa_g = \frac{\kappa_t A_{\frac{1}{2}}(x_t) + \frac{m_t}{M_T}\kappa_T A_{\frac{1}{2}}(x_T) + \frac{m_t}{M_U}\kappa_U A_{\frac{1}{2}}(x_U)}{A_{\frac{1}{2}}(x_t)}, \tag{30}$$

$$\kappa_\gamma = \frac{A_1(x_W) + \frac{4}{3}(\kappa_t A_{\frac{1}{2}}(x_t) + \frac{m_t}{M_T}\kappa_T A_{\frac{1}{2}}(x_T) + \frac{m_t}{M_U}\kappa_U A_{\frac{1}{2}}(x_U))}{A_1(x_W) + \frac{4}{3}A_{\frac{1}{2}}(x_t)}, \tag{31}$$

$$\kappa_t = G^h_{tt}/g^{\rm SM}_{tth}, \qquad g^{\rm SM}_{tth} \equiv \frac{m_t}{v}, \tag{32}$$

$$\kappa_T = G^h_{TT}/g^{\rm SM}_{tth}, \qquad \kappa_U = G^h_{UU}/g^{\rm SM}_{tth}, \tag{33}$$

with $x_i \equiv m_h^2/(4m_i^2)$. The loop functions for spin 1 and 1/2 are represented by $A_1(x)$ and $A_{1/2}(x)$, respectively [41,42],

$$A_1(x) = -\frac{1}{x^2}[2x^2 + 3x + 3(2x-1)f(x)], \tag{34}$$

$$A_{\frac{1}{2}}(x) = \frac{2}{x^2}[x + (x-1)f(x)], \tag{35}$$

with

$$f(x) \equiv \begin{cases} \arcsin^2\sqrt{x} & \text{for} \quad x \le 1, \\ -\frac{1}{4}\left[\ln\frac{1+\sqrt{1-x^{-1}}}{1-\sqrt{1-x^{-1}}} - i\pi\right]^2 & \text{for} \quad x > 1. \end{cases} \tag{36}$$

In our model, the scaling factor κ_V of the hWW and hZZ couplings is SM-like, $\kappa_V = 1$. Since we do not change the down quark and lepton sectors, the scaling factors of the bottom and tau are also $\kappa_b = \kappa_\tau = 1$.

By using the results of the LHC Run 1 via the six-parameter fit shown in Ref. [1],

$$\mu_V/\mu_F = 1.09^{+0.36}_{-0.28}, \tag{37}$$

$$\mu^{\gamma\gamma}_F = 1.10^{+0.23}_{-0.21}, \tag{38}$$

$$\mu^{ZZ}_F = 1.27^{+0.28}_{-0.24}, \tag{39}$$

$$\mu^{WW}_F = 1.06^{+0.21}_{-0.18}, \tag{40}$$

$$\mu^{\tau\tau}_F = 1.05^{+0.33}_{-0.27}, \tag{41}$$

$$\mu^{bb}_F = 0.64^{+0.37}_{-0.28}, \tag{42}$$

we read the 2σ constraints as

$$0.79 < \mu^{VV}_F < 1.48, \qquad 0.68 < \mu^{\gamma\gamma}_F < 1.56, \tag{43}$$

because of $\mu^{WW}_F = \mu^{ZZ}_F \equiv \mu^{VV}_F$ in our model. On the other hand, the best fit values of $(\sigma\cdot B)^{ZZ}_{ggF}$, $\sigma_{VBF}/\sigma_{ggF}$ and $B^{\gamma\gamma}/B^{ZZ}$ yield $\mu^{ZZ}_{ggF} = 1.42^{+0.35}_{-0.31}$ and $\mu^{\gamma\gamma}_{ggF} = 0.67^{+0.25}_{-0.21}$ in the ATLAS Run 2 [43]. The signal strengths in the CMS Run 2 are $\mu^{ZZ}_{ggF} = 1.20^{+0.22}_{-0.21}$ [5] and $\mu^{\gamma\gamma}_{ggF} = 0.77^{+0.25}_{-0.23}$ [3]. One should keep in mind that both of the Run 2 results for $\mu^{\gamma\gamma}_{ggF}$ are much smaller than that of the LHC Run 1.

The parameter space of the mass matrix (4) is constrained by the precision measurements [40]. Especially, owing to the mixing among t, T, and U, the T-parameter is potentially large. We explicitly show the expression of the S and T-parameters in our model in Appendix A [9,10]. Fixing $U = 0$, we impose the constraints [44],

$$\Delta S = 0.07 \pm 0.08, \qquad \Delta T = 0.10 \pm 0.07, \tag{44}$$

where $m_t = 173.3$ GeV, $m_b = 4.2$ GeV, and $m_h = 125.1$ GeV [44].

We now describe the numerical results. In the following analysis, we take the Higgs mass, the pole mass of the top, the $\overline{\rm MS}$ mass of the bottom, and the CKM matrix element for t and b as $m_h = 125.1$ GeV, $m_t^{\rm pole} = 173.2$ GeV, $m_b^{\overline{\rm MS}} = 4.2$ GeV, and $|V_{tb}| = 0.95$, respectively. The relation $m_1 = m_t$ must hold. Although strong couplings are acceptable in our scenario, we may impose $|y_{ij}| < 5$ for the Lagrangian parameters in Eq. (4). Even in this case, there is still wide parameter space, as we will see below. Considering the lower mass bound for the T quark [45], we fix $M_T = 1.2$ TeV and take the mass range for the heavier VLQ to $1.5 \le M_U \le 3.5$ TeV.

The signal strengths of μ^{VV}_F and $\mu^{\gamma\gamma}_F$ are depicted in Figs. 1 and 2. For the red points, the S, T constraints and the 2σ bounds (43) of the Higgs signal strengths are satisfied, while the green points are outside of the 2σ bounds (43). For the blue points in Figs. 1 and 2, $G^h_{tt} > g^{\rm SM}_{tth}$ and $G^h_{TT} > 0$. We did not plot the data with $G^h_{tt} < g^{\rm SM}_{tth}$ in our model, although they exist. We also show the results for MCHM4 and MCHM5, where the scaling parameters are $\kappa_V = \sqrt{1-\xi}$ for both and $\kappa_f = \sqrt{1-\xi}$ and $\kappa_f = (1-2\xi)/\sqrt{1-\xi}$ for MCHM4 and MCHM5, respectively, with $\xi = v^2/f^2$ and f being the typical scale of the MCHMs [25–27,46,47]. The 2σ constraint of the top Yukawa coupling from the Run 1 combined data [1], which reads $1.05 < \kappa_t < 1.92$, is also shown in Figs. 1 and 2 with the proviso that the Run 2 data do not restrict the top Yukawa so much yet, within the 2σ bounds, $0.63 < \kappa_t < 1.79$ (ATLAS Run2 [2]) and $0.71 < \kappa_t < 1.58$ (CMS Run2 [6]). In passing, we comment that there is a parameter space inside of the 2σ bounds (43), even if we take $M_T = 2.0$ TeV. Although the window is closed at $M_T = 2.4$ TeV under the condition $|y_{ij}| < 5$, the parameter space still exists even for $M_T = 3.0$ TeV, if we allow $|y_{ij}| > 5$.

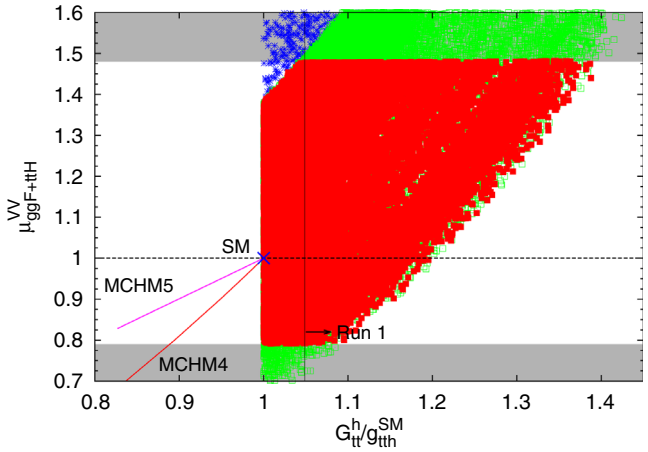

FIG. 1. $\mu^{VV}_{ggF+ttH}$ vs $G^h_{tt}/g^{\rm SM}_{tth}$. We fixed $M_T = 1.2$ TeV and took the mass range, $1.5 \le M_U \le 3.5$ TeV. The upper and lower shaded regions are outside of the 2σ constraints (43). The red points are inside of the 2σ constraints of the LHC Run 1. The green points satisfy only the conditions of $G^h_{tt}/g^{\rm SM}_{tth} > 1$ and $G^h_{TT} < 0$, and the S, T-constraints, while in the blue ones, $G^h_{tt}/g^{\rm SM}_{tth} > 1$ and $G^h_{TT} > 0$. We do not show the results with $G^h_{tt}/g^{\rm SM}_{tth} < 1$ in our model, although they exist. We also show the results for MCHM4 and MCHM5.

In our scenario, we require $G^h_{tt} > g^{\rm SM}_{tth}$ and $G^h_{TT} < 0$ in order for the Higgs signal strengths to be consistent with the experiments. For this cancellation mechanism among the diagonal Yukawa couplings in the gluon fusion process, we show the normalized Yukawa couplings of $\kappa_{T,U} = G^h_{TT,UU}/g^{\rm SM}_{tth}$ vs $\kappa_t = G^h_{tt}/g^{\rm SM}_{tth}$ in Fig. 3. At the red points,

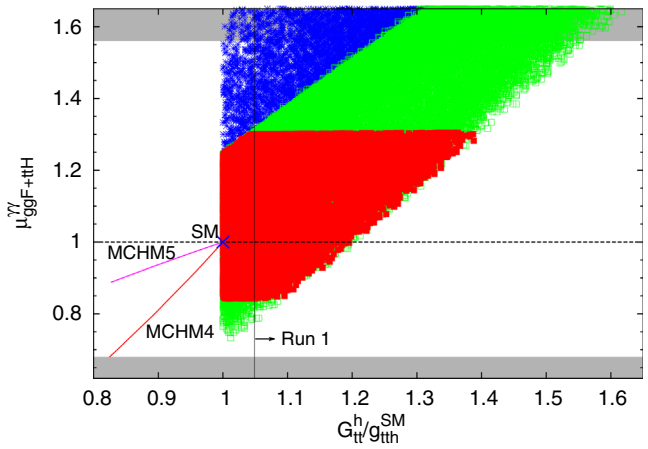

FIG. 2. $\mu^{\gamma\gamma}_{ggF+ttH}$ vs $G^h_{tt}/g^{\rm SM}_{tth}$. We fixed $M_T = 1.2$ TeV and took the mass range, $1.5 \le M_U \le 3.5$ TeV. The upper and lower shaded regions are outside of the 2σ constraints (43). The red points are inside of the 2σ constraints of the LHC Run 1. The green points satisfy only the conditions of $G^h_{tt}/g^{\rm SM}_{tth} > 1$ and $G^h_{TT} < 0$, and the S, T-constraints, while in the blue ones, $G^h_{tt}/g^{\rm SM}_{tth} > 1$ and $G^h_{TT} > 0$. We do not show the results with $G^h_{tt}/g^{\rm SM}_{tth} < 1$ in our model, although they exist. We also show the results for MCHM4 and MCHM5.

the conditions of $G^h_{tt} > g^{\rm SM}_{tth}$ and $G^h_{TT} < 0$, the 2σ constraints (43), and the S, T-constraints (44) are satisfied. On the other hand, the green points are outside of the 2σ constraints (43). We find that the cancellation mechanism works up to $\kappa_t \lesssim 1.4$.

The Lagrangian parameters are important for the model-building. We depict them in Fig. 4. The entry of y_{21} can be either positive or negative. The vanishing y_{21} is also possible. This is consistent with the analytical approach in the previous subsection. Although y_{23} barely takes negative or small positive values, y_{ij} except for y_{21} are positive and large, say, $y_{ij} \gtrsim 2$, in the wide parameter space. Thus the VLQ model discussed here might be provided from some underlying theories based on strongly interacting systems.

In the end of this subsection, we comment on the di-Higgs production via the gluon fusion. The off-diagonal Yukawa couplings can be extracted from the decay channels such as $T \to th$. Also, they contribute to the box diagram of the di-Higgs production, so that the $gg \to hh$ process may give us further information on the model

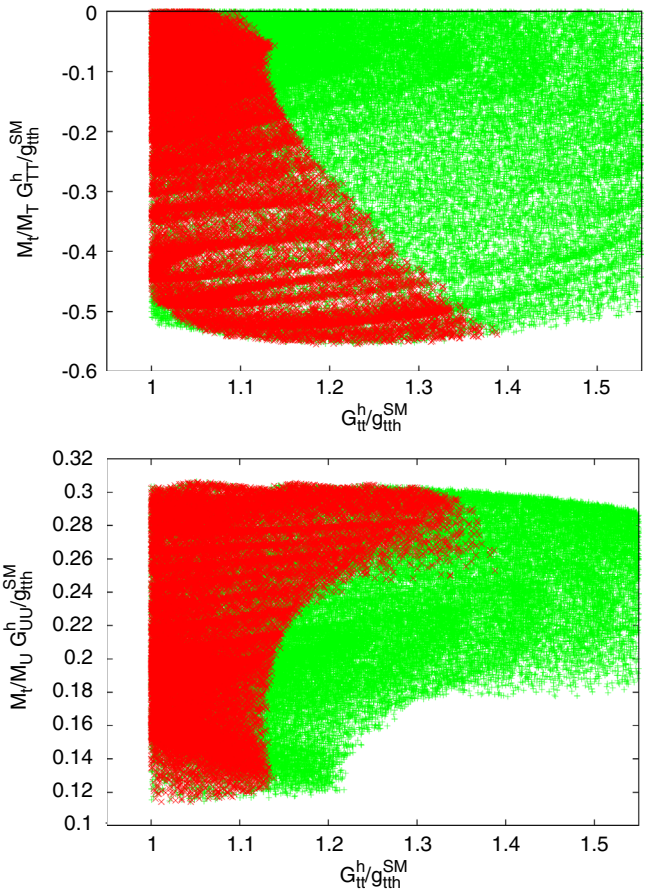

FIG. 3. The diagonal components of the physical Yukawa couplings. The red points are inside of the 2σ constraints (43), while the green points satisfy only the conditions of $G^h_{tt}/g^{\rm SM}_{tth} > 1$ and $G^h_{TT} < 0$, and the S, T-constraints.

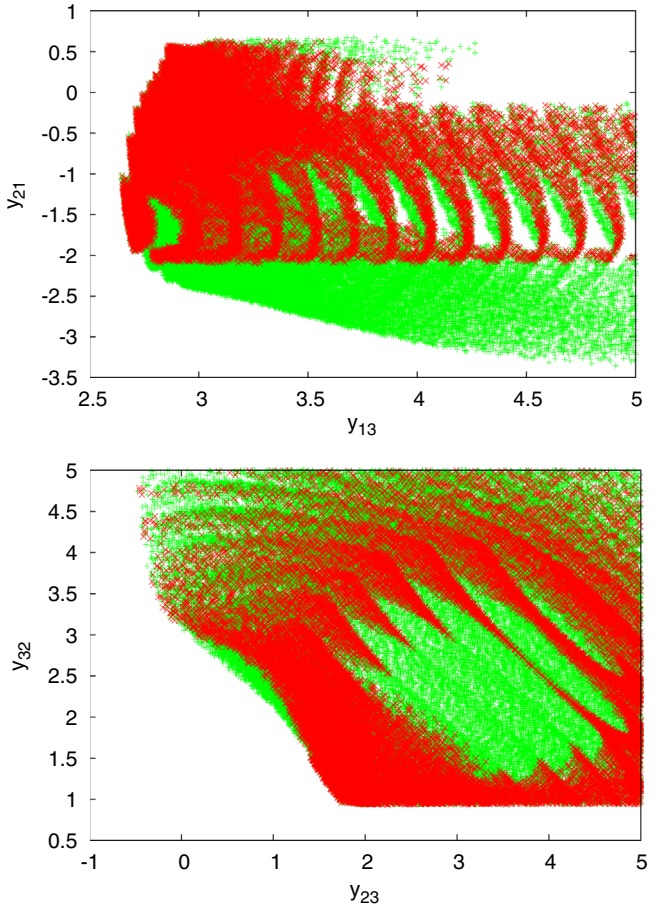

FIG. 4. The Lagrangian parameters of the Yukawa couplings in Eq. (4). The red points are inside of the 2σ constraints (43), while the green points satisfy only the conditions of $G^h_{tt}/g^{\rm SM}_{tth} > 1$ and $G^h_{TT} < 0$, and the S, T-constraints.

parameters. In the lowest order of the $1/M$ expansion (LET), the triangle and box contributions normalized by the SM values are [32–34,36–38]

$$R^{\rm tri}_{gg\to h} = \frac{\mathcal{A}_{gg\to h}}{\mathcal{A}^{\rm SM}_{gg\to h}} = v{\rm Tr}(\mathbf{G}^h\mathcal{M}^{-1}_{\rm diag}), \tag{45}$$

$$R^{\rm box}_{gg\to hh} = \frac{\mathcal{A}^{\rm box}_{gg\to hh}}{\mathcal{A}^{\rm SM,box}_{gg\to hh}} = v^2{\rm Tr}(\mathbf{G}^h\mathcal{M}^{-1}_{\rm diag}\mathbf{G}^h\mathcal{M}^{-1}_{\rm diag}), \tag{46}$$

respectively. Note that $R^{\rm tri}_{gg\to h} \approx \kappa_g$, because of $A_{\frac{1}{2}}(x_t) \simeq A_{\frac{1}{2}}(x_T) \simeq A_{\frac{1}{2}}(x_U) \approx A_{\frac{1}{2}}(0) = 4/3$. The numerical result is depicted in Fig. 5. Also, we can analytically obtain the expressions of $R^{\rm tri}_{gg\to h}$ and $R^{\rm box}_{gg\to hh}$ in the general case (4) as

$$\begin{aligned} R^{\rm tri}_{gg\to h} &= 3 - 2b_{22}, \\ R^{\rm box}_{gg\to hh} &= 3 - 6b_{22} + 4b^2_{22} = (R^{\rm tri}_{gg\to h})^2 - 3(R^{\rm tri}_{gg\to h} - 1), \end{aligned} \tag{47}$$

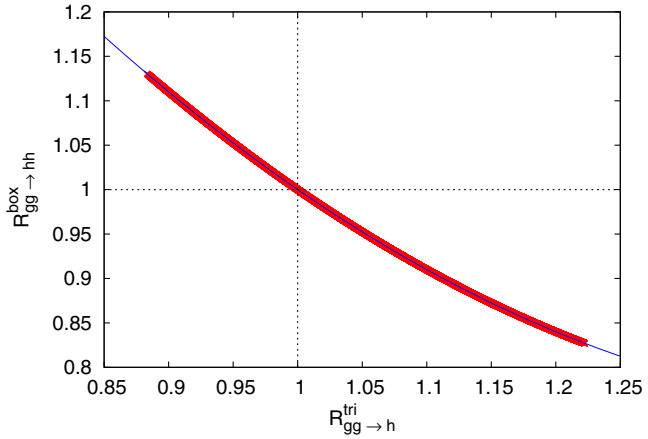

FIG. 5. $R^{\rm tri}_{gg\to h}$ vs $R^{\rm box}_{gg\to hh}$. The red points are inside of the 2σ constraints (43). The blue curve corresponds to the analytical relation, $R^{\rm box}_{gg\to hh} = (R^{\rm tri}_{gg\to h})^2 - 3(R^{\rm tri}_{gg\to h} - 1)$, shown in Eq. (47).

where b_{22} denotes the (2,2) element of the dimensionless mass matrix inverse $M_X\mathcal{M}^{-1}$. See also Appendix B. This analytic result is shown as the blue curve in Fig. 5. Under the symmetric mass matrix assumption (9) in the previous subsection, we find $R^{\rm tri}_{gg\to h} = R^{\rm box}_{gg\to hh} = 1$ owing to $b_{22} = 1$. It then turns out that the box contribution $R^{\rm box}_{gg\to hh}$ is decreasing with respect to the increasing triangle contribution $R^{\rm tri}_{gg\to h}$ under the 2σ constraints (43). Since the box is destructive in $gg \to hh$, it means that the di-Higgs production is either much enhanced or suppressed. In Fig. 6, we show the ratio $\sigma_{\rm LET}/\sigma^{\rm SM}_{\rm LET}$ of the total cross section of the Higgs pair production through gg in pp collisions normalized by the SM one under the LET approximation [32–34,36–38]. We took the LHC center of mass energy as $\sqrt{s} = 14$ TeV and used the CT14 LO PDF set [48]. The

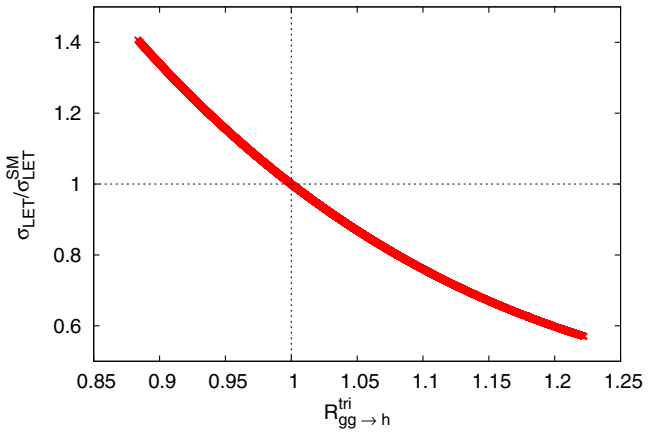

FIG. 6. The ratio $\sigma_{\rm LET}/\sigma^{\rm SM}_{\rm LET}$ of the total $pp \to hh$ cross section at $\sqrt{s} = 14$ TeV normalized by the SM value under the LET approximation. We used the CT14 LO PDF set [48] and took the renormalization and factorization scales equal to the invariant mass of the Higgs pair, $\mu = Q = M_{hh} = \sqrt{\hat{s}}$.

renormalization scale (μ) and the factorization scale (Q) are chosen equal to the invariant mass ($M_{hh} = \sqrt{\hat{s}}$) of the Higgs pair, $\mu = Q = M_{hh}$. We find that the ratio can be increasing/decreasing about 40%, depending on the values of $R^{\rm tri}_{gg\to h} \approx \kappa_g$. This might be striking, although one should take notice of inaccuracy of the LET approximation. A detailed analysis will be performed elsewhere.

IV. SUMMARY AND DISCUSSIONS

We revisited the scenario with the enhanced top Yukawa coupling in the framework of the VLQ model. We found that the scenario can be realized in the rather wide parameter space. Since the Lagrangian parameters of the Yukawa couplings except for y_{21} are positive and large, such VLQ model can be obtained from some underlying strong dynamics. We also calculated the ratios of the triangle and box diagrams to the SM values in the $gg \to hh$ process and found the noticeable relation. The detailed studies will be done in the future.

ACKNOWLEDGMENTS

The author thank to A. Deandrea and G. Cacciapaglia for useful comments. Numerical computation in this work was carried out at the Yukawa Institute Computer Facility. This work is supported by JSPS Grant-in-Aid for Scientific Research No. 17K05423 and partially by the France-Japan Particle Physics Lab (TYL/FJPPL).

APPENDIX A: S, T-PARAMETERS IN THE VLQ MODEL

The parameter space of the VLQ models is severely restricted by the oblique corrections [40]. In particular, the T-parameter is essential. In our model, it reads [9,10],

$$
\begin{aligned}
T = \frac{N_c}{16\pi s_W^2 c_W^2}\Bigg[&\sum_{k=1}^{3}(|L_{1k}|^2\theta_+(y_k,y_b) + (|L_{2k}|^2+|R_{2k}|^2)\theta_+(y_X,y_k) + 2{\rm Re}(L_{2k}R_{2k}^*)\theta_-(y_X,y_k)) - \frac{1}{2}\theta_+(y_b,y_b)\\
&- \theta_+(y_X,y_X) - \theta_-(y_X,y_X) - \sum_{k=1}^{3}\left\{\frac{1}{2}((|L_{1k}|^2-|L_{2k}|^2)^2+|R_{2k}|^4)\theta_+(y_k,y_k) - (|L_{1k}|^2-|L_{2k}|^2)|R_{2k}|^2\theta_-(y_k,y_k)\right\}\\
&- \sum_{i\neq j}\left\{\frac{1}{2}(|L_{1i}^*L_{1j}-L_{2i}^*L_{2j}|^2+|R_{2i}^*R_{2j}|^2)\theta_+(y_i,y_j) - {\rm Re}((L_{1i}^*L_{1j}-L_{2i}^*L_{2j})R_{2i}R_{2j}^*)\theta_-(y_i,y_j)\right\}\Bigg],
\end{aligned}
\tag{A1}
$$

where $N_c = 3$, and we defined $s_W \equiv \sin\theta_W$ and $c_W \equiv \cos\theta_W$ with θ_W being the weak mixing angle, and also

$$
y_i \equiv \frac{m_i^2}{m_Z^2}, \qquad y_b \equiv \frac{m_b^2}{m_Z^2}, \qquad y_X \equiv \frac{M_X^2}{m_Z^2}, \tag{A2}
$$

$$
\begin{aligned}
\theta_+(y_i,y_j) \equiv\ & y_i + y_j - \frac{2y_iy_j}{y_i-y_j}\log\frac{y_i}{y_j}\\
&- 2(y_i\log y_i + y_j\log y_j) + \frac{y_i+y_j}{2}\Delta,
\end{aligned}
\tag{A3}
$$

and

$$
\theta_-(y_i,y_j) \equiv 2\sqrt{y_iy_j}\left(\frac{y_i+y_j}{y_i-y_j}\log\frac{y_i}{y_j} - 2 + \log(y_iy_j) - \frac{\Delta}{2}\right), \tag{A4}
$$

with Δ being the divergent term in the dimensional regularization. The mass eigenvalues of the up-type quarks are $m_1 = m_t$, $m_2 = M_T$, and $m_3 = M_U$. The rotation matrices are defined by

$$
\begin{aligned}
\begin{pmatrix} t_L \\ T_L \\ U_L \end{pmatrix} &= \begin{pmatrix} L_{11} & L_{12} & L_{13} \\ L_{21} & L_{22} & L_{23} \\ L_{31} & L_{32} & L_{33} \end{pmatrix}\begin{pmatrix} t'_L \\ T'_L \\ U'_L \end{pmatrix},\\
\begin{pmatrix} t_R \\ T_R \\ U_R \end{pmatrix} &= \begin{pmatrix} R_{11} & R_{12} & R_{13} \\ R_{21} & R_{22} & R_{23} \\ R_{31} & R_{32} & R_{33} \end{pmatrix}\begin{pmatrix} t'_R \\ T'_R \\ U'_R \end{pmatrix},
\end{aligned}
\tag{A5}
$$

where $(t,T,U)_{L,R}$ and $(t',t',U')_{L,R}$ are the gauge and mass eigenstates, respectively.

We have left the divergent term Δ for checking of the calculations [10]. By using the unitarity and the mass relations

$$
\begin{aligned}
M_X = \mathcal{M}_{22} &= (V_L{\rm diag}(m_1,m_2,m_3)V_R^\dagger)_{22}\\
&= m_1L_{21}R_{21}^* + m_2L_{22}R_{22}^* + m_3L_{23}R_{23}^*,
\end{aligned}
\tag{A6}
$$

and also

$$
\begin{aligned}
0 = \mathcal{M}_{12} &= (V_L{\rm diag}(m_1,m_2,m_3)V_R^\dagger)_{12}\\
&= m_1L_{11}R_{21}^* + m_2L_{12}R_{22}^* + m_3L_{13}R_{23}^*,
\end{aligned}
\tag{A7}
$$

we can confirm that the divergent term Δ is exactly canceled out, as it must be.

The deviation from the SM is given by

$$\Delta T = T - T_{\rm SM}, \tag{A8}$$

with

$$T_{\rm SM} = \frac{N_c}{16\pi s_W^2 c_W^2 m_Z^2}\left[m_t^2 + m_b^2 - 2\frac{m_t^2 m_b^2}{m_t^2 - m_b^2}\log\frac{m_t^2}{m_b^2}\right]. \tag{A9}$$

Throughout the paper, we take the 1σ constraint, $\Delta T = 0.10 \pm 0.07$ [44].

The S-parameter constraint is not so severe, compared with the T-parameter. The expression for the S-parameter in our model is as follows [9]:

$$\begin{aligned} S = \frac{N_c}{2\pi}\Bigg[&\sum_{k=1}^{3}(|L_{1k}|^2\psi_+(y_k,y_b) + (|L_{2k}|^2 + |R_{2k}|^2)\psi_+(y_X,y_k) \\ &+ 2{\rm Re}(L_{2k}R_{2k}^*)\psi_-(y_X,y_k)) \\ &- \sum_{i\neq j}\Bigg\{\frac{1}{2}(|L_{1i}^* L_{1j} - L_{2i}^* L_{2j}|^2 + |R_{2i}^* R_{2j}|^2)\chi_+(y_i,y_j) \\ &- {\rm Re}((L_{1i}^* L_{1j} - L_{2i}^* L_{2j})R_{2i}R_{2j}^*)\chi_-(y_i,y_j)\Bigg\}\Bigg], \end{aligned} \tag{A10}$$

where we defined

$$\psi_+(y_i,y_j) \equiv \frac{1}{3} - \frac{1}{9}\log\frac{y_i}{y_j}, \tag{A11}$$

$$\psi_-(y_i,y_j) \equiv -\frac{y_i + y_j}{6\sqrt{y_i y_j}}, \tag{A12}$$

$$\begin{aligned} \chi_+(y_i,y_j) \equiv &\frac{5(y_i^2 + y_j^2) - 22 y_i y_j}{9(y_i - y_j)^2} \\ &+ \frac{3y_i y_j(y_i + y_j) - y_i^3 - y_j^3}{3(y_i - y_j)^3}\log\frac{y_i}{y_j}, \end{aligned} \tag{A13}$$

and

$$\begin{aligned} \chi_-(y_i,y_j) \equiv -\sqrt{y_i y_j}\Bigg(&\frac{y_i + y_j}{6y_i y_j} - \frac{y_i + y_j}{(y_i - y_j)^2} \\ &+ \frac{2y_i y_j}{(y_i - y_j)^3}\log\frac{y_i}{y_j}\Bigg). \end{aligned} \tag{A14}$$

Note that $\chi_+(y_i,y_i) = \chi_-(y_i,y_i) = 0$.

The deviation from the SM is given by

$$\Delta S = S - S_{\rm SM}, \tag{A15}$$

with

$$S_{\rm SM} = \frac{N_c}{2\pi}\left[\frac{1}{3} - \frac{1}{9}\log\frac{m_t^2}{m_b^2}\right]. \tag{A16}$$

Throughout the paper, we take the 1σ constraint, $\Delta S = 0.07 \pm 0.08$ [44].

APPENDIX B: ANALYTICAL EXPRESSION OF $R_{gg\to h}^{\rm tri}$ AND $R_{gg\to hh}^{\rm box}$

For the general mass matrix (4) in our model, we define the dimensionless matrices as follows:

$$\begin{aligned} \widetilde{\mathcal{M}} &\equiv \frac{1}{M_X}\mathcal{M} = \begin{pmatrix} 0 & 0 & a_{13} \\ a_{21} & 1 & a_{23} \\ a_{31} & a_{32} & a_{33} \end{pmatrix}, \\ \widetilde{\mathbf{Y}} &\equiv \frac{1}{\sqrt{2}}\frac{v}{M_X}\mathbf{Y} = \begin{pmatrix} 0 & 0 & a_{13} \\ a_{21} & 0 & a_{23} \\ 0 & a_{32} & 0 \end{pmatrix}, \end{aligned} \tag{B1}$$

where we scaled by $M_X = m_{22}$. We assume $a_{13} \neq 0$ for getting $m_t \neq 0$. We then read Eqs. (45) and (46) as

$$R_{gg\to h}^{\rm tri} = {\rm tr}(\widetilde{\mathbf{Y}}\widetilde{\mathcal{M}}^{-1}), \quad R_{gg\to hh}^{\rm box} = {\rm tr}(\widetilde{\mathbf{Y}}\widetilde{\mathcal{M}}^{-1}\widetilde{\mathbf{Y}}\widetilde{\mathcal{M}}^{-1}). \tag{B2}$$

Let us determine the dimensionless mass matrix inverse $\widetilde{\mathcal{M}}^{-1}$. The definition of the inverse matrix, $\widetilde{\mathcal{M}}\widetilde{\mathcal{M}}^{-1} = \widetilde{\mathcal{M}}^{-1}\widetilde{\mathcal{M}} = {\rm diag}(1,1,1)$, yields the expression for $\widetilde{\mathcal{M}}^{-1}$ as

$$\widetilde{\mathcal{M}}^{-1} = \begin{pmatrix} b_{11} & b_{12} & b_{13} \\ b_{21} & b_{22} & b_{23} \\ \frac{1}{a_{13}} & 0 & 0 \end{pmatrix}, \tag{B3}$$

and the matrix elements b_{ij} satisfy

$$\begin{aligned} \begin{pmatrix} a_{21} & 1 \\ a_{31} & a_{32} \end{pmatrix}\begin{pmatrix} b_{12} & b_{13} \\ b_{22} & b_{23} \end{pmatrix} &= \begin{pmatrix} 1 & 0 \\ 0 & 1 \end{pmatrix}, \\ \begin{pmatrix} a_{21} & 1 \\ a_{31} & a_{32} \end{pmatrix}\begin{pmatrix} b_{11} \\ b_{21} \end{pmatrix} &= -\frac{1}{a_{13}}\begin{pmatrix} a_{23} \\ a_{33} \end{pmatrix}. \end{aligned} \tag{B4}$$

Therefore we analytically obtain b_{ij},

$$\begin{pmatrix} b_{12} & b_{13} \\ b_{22} & b_{23} \end{pmatrix} = \frac{1}{a_{21}a_{32} - a_{31}}\begin{pmatrix} a_{32} & -1 \\ -a_{31} & a_{21} \end{pmatrix}, \tag{B5}$$

and

$$\begin{pmatrix} b_{11} \\ b_{21} \end{pmatrix} = -\frac{1}{a_{13}(a_{21}a_{32} - a_{31})}\begin{pmatrix} a_{32}a_{23} - a_{33} \\ -a_{31}a_{23} + a_{21}a_{33} \end{pmatrix}. \tag{B6}$$

By using $a_{21}b_{12} = a_{32}b_{23} = 1 - b_{22}$, we find

$$R^{\text{tri}}_{gg\to h} = 3 - 2b_{22}, \tag{B7}$$

and

$$\begin{aligned} R^{\text{box}}_{gg\to hh} &= 1 + 2(1 - b_{22})^2 - 2b_{22}(1 - b_{22}) \\ &= 3 - 6b_{22} + 4b_{22}^2. \end{aligned} \tag{B8}$$

Eliminating b_{22} from the above equations, we obtain Eq. (47),

$$R^{\text{box}}_{gg\to hh} = (R^{\text{tri}}_{gg\to h})^2 - 3(R^{\text{tri}}_{gg\to h} - 1). \tag{B9}$$

When $a_{21} = 0$ as in Sec. III A, we immediately find $b_{22} = 1$ and thereby obtain $R^{\text{tri}}_{gg\to h} = R^{\text{box}}_{gg\to hh} = 1$.

[1] G. Aad *et al.* (ATLAS and CMS Collaborations), Measurements of the Higgs boson production and decay rates and constraints on its couplings from a combined ATLAS and CMS analysis of the LHC pp collision data at $\sqrt{s} =$ 7 and 8 TeV, J. High Energy Phys. 08 (2016) 045.

[2] The ATLAS Collaboration, Report No. ATLAS-CONF-2016-068.

[3] CMS Collaboration, Report No. CMS-PAS-HIG-16-020.

[4] CMS Collaboration, Report No. CMS-PAS-HIG-16-038.

[5] CMS Collaboration, Report No. CMS-PAS-HIG-16-041.

[6] CMS Collaboration, Report No. CMS-PAS-HIG-17-004.

[7] V. A. Miransky, M. Tanabashi, and K. Yamawaki, Dynamical electroweak symmetry breaking with large anomalous dimension and t quark condensate, Phys. Lett. B **221**, 177 (1989); Is the t quark responsible for the mass of w and z bosons, Mod. Phys. Lett. A **04**, 1043 (1989); Y. Nambu, Enrico Fermi Institute Report No. 89-08, 1989; in *Proceedings of the 1988 Kazimierz Workshop*, edited by Z. Ajduk *et al.* (World Scientific, Singapore, 1989); W. A. Bardeen, C. T. Hill, and M. Lindner, Minimal dynamical symmetry breaking of the standard model, Phys. Rev. D **41**, 1647 (1990).

[8] B. Holdom, Heavy Quarks And Electroweak Symmetry Breaking, Phys. Rev. Lett. **57**, 2496 (1986); Errattum, Phys. Rev. Lett. **58**, 177(E) (1987); G. D. Kribs, T. Plehn, M. Spannowsky, and T. M. P. Tait, Four generations and Higgs physics, Phys. Rev. D **76**, 075016 (2007); M. Hashimoto, Constraints on mass spectrum of fourth generation fermions and Higgs bosons, Phys. Rev. D **81**, 075023 (2010); For a review, see, P. H. Frampton, P. Q. Hung, and M. Sher, Quarks and leptons beyond the third generation, Phys. Rep. **330**, 263 (2000).

[9] L. Lavoura and J. P. Silva, The oblique corrections from vectorlike singlet and doublet quarks, Phys. Rev. D **47**, 2046 (1993).

[10] C. Anastasiou, E. Furlan, and J. Santiago, Realistic composite Higgs models, Phys. Rev. D **79**, 075003 (2009).

[11] G. Cacciapaglia, A. Deandrea, D. Harada, and Y. Okada, Bounds and decays of new heavy vector-like top partners, J. High Energy Phys. 11 (2010) 159.

[12] G. Cacciapaglia, A. Deandrea, L. Panizzi, N. Gaur, D. Harada, and Y. Okada, Heavy vector-like top partners at the LHC and flavour constraints, J. High Energy Phys. 03 (2012) 070.

[13] J. A. Aguilar-Saavedra, R. Benbrik, S. Heinemeyer, and M. Pérez-Victoria, Handbook of vectorlike quarks: Mixing and single production, Phys. Rev. D **88**, 094010 (2013).

[14] A. K. Alok, S. Banerjee, D. Kumar, S. U. Sankar, and D. London, New-physics signals of a model with a vector-singlet up-type quark, Phys. Rev. D **92**, 013002 (2015).

[15] A. K. Alok, S. Banerjee, D. Kumar, and S. Uma Sankar, Flavor signatures of isosinglet vector-like down quark model, Nucl. Phys. **B906**, 321 (2016).

[16] G. Cacciapaglia, A. Deandrea, N. Gaur, D. Harada, Y. Okada, and L. Panizzi, Interplay of vector-like top partner multiplets in a realistic mixing set-up, J. High Energy Phys. 09 (2015) 012.

[17] A. Angelescu, A. Djouadi, and G. Moreau, Vector-like top/bottom quark partners and Higgs physics at the LHC, Eur. Phys. J. C **76**, 99 (2016).

[18] A. Biekötter, J. L. Hewett, J. S. Kim, M. Krämer, T. G. Rizzo, K. Rolbiecki, J. Tattersall, and T. Weber, Complementarity of resonant scalar, vector-like quark and superpartner searches in elucidating new phenomena, Int. J. Mod. Phys. A **32**, 1750032 (2017).

[19] C. Y. Chen, S. Dawson, and E. Furlan, Vector-like fermions and Higgs effective field theory revisited, Phys. Rev. D **96**, 015006 (2017).

[20] K. Agashe, R. Contino, and A. Pomarol, The minimal composite Higgs model, Nucl. Phys. **B719**, 165 (2005).

[21] R. Contino, L. Da Rold, and A. Pomarol, Light custodians in natural composite Higgs models, Phys. Rev. D **75**, 055014 (2007).

[22] N. Arkani-Hamed, A. G. Cohen, E. Katz, and A. E. Nelson, The littlest Higgs, J. High Energy Phys. 07 (2002) 034.

[23] M. Schmaltz and D. Tucker-Smith, Little Higgs review, Annu. Rev. Nucl. Part. Sci. **55**, 229 (2005).

[24] B. A. Dobrescu and C. T. Hill, Electroweak Symmetry Breaking via Top Condensation Seesaw, Phys. Rev. Lett. **81**, 2634 (1998); R. S. Chivukula, B. A. Dobrescu, H. Georgi, and C. T. Hill, Top quark seesaw theory of electroweak symmetry breaking, Phys. Rev. D **59**, 075003 (1999); For a review see, e.g., C. T. Hill and E. H. Simmons, Strong dynamics and electroweak symmetry breaking, Phys. Rep. **381**, 235 (2003); Errattum, Phys. Rep.**390**, 553(E) (2004).

[25] D. Liu, I. Low, and C. E. M. Wagner, Modification of Higgs couplings in minimal composite models, arXiv:1703.07791.

[26] J. R. Espinosa, C. Grojean, and M. Muhlleitner, Composite Higgs search at the LHC, J. High Energy Phys. 05 (2010) 065.
[27] M. Carena, L. Da Rold, and E. Pontón, Minimal composite Higgs models at the LHC, J. High Energy Phys. 06 (2014) 159.
[28] H. C. Cheng and J. Gu, Top seesaw with a custodial symmetry, and the 126 GeV Higgs, J. High Energy Phys. 10 (2014) 002.
[29] M. Badziak and C. E. M. Wagner, Enhancing the Higgs associated production with a top quark pair, J. High Energy Phys. 05 (2016) 123.
[30] M. Badziak and C. E. M. Wagner, Enhanced Higgs associated production with a top quark pair in the NMSSM with light singlets, J. High Energy Phys. 02 (2017) 050.
[31] A. Das, N. Maru, and N. Okada, Anomalous Higgs Yukawa couplings and recent LHC data, arXiv:1704.01353.
[32] B. A. Kniehl and M. Spira, Low-energy theorems in Higgs physics, Z. Phys. C **69**, 77 (1995).
[33] A. Falkowski, Pseudo-goldstone Higgs production via gluon fusion, Phys. Rev. D **77**, 055018 (2008).
[34] I. Low, R. Rattazzi, and A. Vichi, Theoretical constraints on the Higgs effective couplings, J. High Energy Phys. 04 (2010) 126.
[35] R. Gröber and M. Mühlleitner, Composite Higgs boson pair production at the LHC, J. High Energy Phys. 06 (2011) 020.
[36] M. Gillioz, R. Gröber, C. Grojean, M. Mühlleitner, and E. Salvioni, Higgs low-energy theorem (and its corrections) in composite models, J. High Energy Phys. 10 (2012) 004.
[37] S. Dawson, E. Furlan, and I. Lewis, Unravelling an extended quark sector through multiple Higgs production?, Phys. Rev. D **87**, 014007 (2013).
[38] C. Y. Chen, S. Dawson, and I. M. Lewis, Top partners and Higgs boson production, Phys. Rev. D **90**, 035016 (2014).
[39] R. Gröber, M. Mühlleitner, and M. Spira, Signs of Composite Higgs pair production at next-to-leading order, J. High Energy Phys. 06 (2016) 080.
[40] M. E. Peskin and T. Takeuchi, A New Constraint on a Strongly Interacting Higgs Sector, Phys. Rev. Lett. **65**, 964 (1990); Estimation of oblique electroweak corrections, Phys. Rev. D **46**, 381 (1992).
[41] J. F. Gunion, H. E. Haber, G. L. Kane, and S. Dawson, The Higgs hunter's guide, Front. Phys. **80**, 1 (2000).
[42] A. Djouadi, The anatomy of electro-weak symmetry breaking. I: The Higgs boson in the standard model, Phys. Rep. **457**, 1 (2008).
[43] The ATLAS collaboration, Report No. ATLAS-CONF-2016-081.
[44] C. Patrignani *et al.* (Particle Data Group), Review of particle physics, Chin. Phys. C **40**, 100001 (2016).
[45] The ATLAS Collaboration, Report No. ATLAS-CONF-2016-104.
[46] S. Kanemura, K. Kaneta, N. Machida, S. Odori, and T. Shindou, Single and double production of the Higgs boson at hadron and lepton colliders in minimal composite Higgs models, Phys. Rev. D **94**, 015028 (2016).
[47] V. Sanz and J. Setford, Composite Higgs models after Run2, arXiv:1703.10190.
[48] S. Dulat, T.-J. Hou, J. Gao, M. Guzzi, J. Huston, P. Nadolsky, J. Pumplin, C. Schmidt, D. Stump, and C.-P. Yuan, New parton distribution functions from a global analysis of quantum chromodynamics, Phys. Rev. D **93**, 033006 (2016).